Softwood-lignin/natural rubber composites containing novel plasticizing agent: Preparation and characterization

Janusz Datta*, Paulina Parcheta, Joanna Surówka

Gdańsk University of Technology, Faculty of Chemistry, Department of Polymers Technology, G. Narutowicza Str. 11/12, 80-233 Gdańsk, Poland

*Corresponding author (J. Datta): janusz.datta@pg.gda.pl

ABSTRACT: Composite materials based on natural rubber were obtained by using glycerolysate (decomposition product of polyurethane) as a novel plasticizer. In order to determine the effect of various lignin content, four different filler amounts were used, namely 5 phr (parts per 100 parts of natural rubber) of lignin (WLI5G), 10 phr of lignin (WLI10G), 20 phr (WLI20G), and 40 phr (WLI40G). The reference specimen without lignin (WLI0G) was also prepared. The resulting vulcanizates were analyzed by Fourier Transform Infrared Spectroscopy (FTIR) to determine the chemical interaction between the lignin powder and the natural rubber chain. The SEM analysis of the cross-sections of the obtained materials was carried out to determine the adhesion between lignin and rubber. The results of dynamic mechanical analysis (DMA) and thermogravimetric analysis (TGA) showed that the samples containing 5 and 10 phr of lignin had the best thermal properties. Also, the measured mechanical properties, such as tensile strength, hardness, resilience and abrasiveness, confirmed these findings.

KEYWORDS:

Softwood Lignin;

Natural rubber composites;
Scanning Electron Microscopy;
Thermal analysis;
Mechanical properties;
Equilibrium swelling measurements

1. INTRODUCTION

At present, many scientific teams work on the possibility to employ natural resources in the field of materials science and engineering. It is a consequence of the ending stocks of petrochemical resources such as coal, natural gas, and crude oil. One of the most important issues related to green chemistry is the utilization of renewable resources as a new application in the existing products. Moreover, the polymer recycling process and the utilization of polymer recycling products constitute the second most urgent task due to the increase in the waste quantity. It has been proven that the renewables and the products of polymer recycling can partially replace the primary resources used in the polymer synthesis and preparation. The resulting materials display the same, approximately the same, or even better properties.

One of the most recent issues in green chemistry is finding the possibility to maximize the application of lignin by-products, which are produced in vast amounts by the paper and pulp industries, in the field of polymer technology. Presently, ca. 50 million tons of lignin by-products produced annually by the industries are used as a fuel for the energy production (Faruket al., 2016a). Only 2 % of this valuable raw material is used for other applications because of the complex structure and heterogeneity of lignin, which causes difficulties during delignification on a commercial scale that is conducted by the pulp and paper industries (DeWild et al., 2014; Neutelings, 2011).

Lignin is a highly branched bio-macromolecule. It is composed of units such as paracoumaryl alcohol, coniferyl alcohol and sinapyl alcohol (Jianget al., 2014). These phenylpropane units have none, one, or two methoxyl groups at the positions 3 or 5 in the phenolic ring (Faruket al., 2016a). The aforementioned molecules are linked together by different bond types, i.e. 5-O-4, β-O-4, β-1, β-5, β-β, etc. (Rogers, 2015). Chakar et al. (Chakarand Ragauskas, 2004) presented the percentages of different bonds in softwood lignin, β-O-4 being the most common one. This particular bond type is present in up to 50 % of total bonds in softwood-lignin.

The varying occurrence of bond types depends on the origin of lignin, i.e. the sources of softwood or hardwood, which results in different percentages of bond content.Bjornsson indicated that generally hardwoods contain less lignin than softwoods (Bjornsson, 2014). The exact lignin structure not only depends of the type of biomass, but also of the type of delignification process used, which modifies lignin to a certain degree (Hatakeyama and Hatakeyama, 2010). The application of various delignification methods results in a variety of lignin products. The main types of lignin can be divided into lignosulfonates, kraft lignin, and organosolv lignin (Holladay et al., 2007).

The delignification process affects the content of impurities in the obtained products and, consequently, their further applicability. Lignosulfonates can be used as dispersants, emulsion stabilizer, carbon black, industrial binders, agricultural chemicals or concrete additives due to their medium purity (residual sulfur). Kraft lignin also contains some ash and sulfur, and can be used as emulsifiers, dispersants, carbon fibers or binders. Organosolv lignin, which is sulfur free, has the highest degree of purity. Because of this property, it is possible to use organosolv lignin for the synthesis of aromatic polyols, new diacids, carbon fibers, activated carbon, phenolic resins, phenol derivatives and antioxidants (Faruket al., 2016a; Holladay et al., 2007).

Plasticizers, represented by freely available, non-volatile compounds, are widely used in the polymer production due to the important role they play in the resulting products. They improve processability during the polymer preparation as well as add flexibility to the final materials (Vieiraet al., 2011). Over the past years, due to the increasing interest of polymer industries in biopolymers, biorenewables and the products of the chemical recycling of polymer waste, many publications appeared in which the addition of a biopolymer plasticizer and/or biodegradable plasticizing materials of natural origin had been described. Altenhofen Da Silva and co-workers utilized the product of the polyesterification of rice fatty acid as a plasticizer in the poly(vinyl chloride) and natural rubber films. The results of this research indicate that the addition of natural plasticizer increased the elongation at break compared to pure polymer film. In terms of thermogravimetric analysis no significant differences were detected between the plasticized material and pure natural rubber-based product (Altenhofen Da Silva et al., 2011). Alexander and Thachil investigated differences between cardanol and aromatic oil emloyed as plasticizers. It was demonstrated that cardanol, used as a plasticizing agent in the natural-rubber matrix, gave mechanical properties similar to those obtained with the aromatic oil-based materials (Alexander and Thachil, 2006). The same observation was later reported by Mohapatra and Nando(Mohapatra and Nando, 2014).

The main aim of this research was to prepare and characterize natural rubber-based composites filled with various amounts of lignin, and obtained with the use of glycerolysate. This experimental set up was an exemplification of the application of the chemical recycling of polymer product as a novel plasticizer in the natural rubber matrix. The synthesis of the plasticizer used in our study had been based on the decomposition of polyurethane waste by means of chemicals, heat and catalysts. Polyurethanes are in the sixth place in the ranking of the most used polymers in the global market. The polyurethane waste constitutes ca. 6 % of all plastic waste (Kopczyńska and Datta, 2016). As a result, the chemical recycling processes of polyurethanes are one of the most prolific development tasks in the materials engineering (Simonet al., 2014). Moreover, the most investigated are the wastes of flexible polyurethane foams due to their extensive application and the resulting high volume of waste that entails environmental and economic problems (Nikjeand Nikrah, 2007). Glycerolysate is the product of thermo-mechanical recycling of polyurethane, with the use of glycerine as a decomposition prime mover. The process is called glycolysis or glycerolysis, and it is the transesterification reaction between hydroxyl groups in glycol or glycerol (glycerine), respectively, which interchanged the ester groups in the polyurethane chains (Simónet al., 2016). The decomposition product of polyurethane is a mixture of compounds and monomers. Until now, glycerolysates were most frequently used to synthesize polyurethanes, mainly in the form of foams (Simónet al., 2016) or elastomers (Datta,2010; Datta and Pasternak, 2005), in which polyols were partially or completely replaced by the product of the chemical recycling of polyurethane.

This paper describes novel elastic composites containing four different levels of lignin, and the same amount of plasticizer in the form of glycerolysate. The influence of lignin content on the structure, morphology, and the selected mechanical, thermal and chemical properties of the obtained composites was investigated.

2. EXPERIMENTAL

2.1. MATERIALS

Natural rubber used to prepare the composites was purchased from Torimex Chemicals Ltd Sp. z o. o., KonstantynówŁódzki, Poland (density 0.92 g/cm^3, weight average molecular weight, M_w = 800 000 mol/g). Lignin (INDULIN AT – kraft pine lignin – softwood lignin) used in this study was obtained from MeadWestvaco Corporation, Specialty Chemical Division, South Carolina, USA. INDULIN AT with a density of ca. 1.25 g/cm^3 was dried prior to use at 100^{o}C for 12 hours in air. After drying, it was applied as a filler in the rubber mix. Sulfur with a density of about 1.8-2.1 g/cm^3 and a molecular weight of 32.1 g/mol was also purchased from Torimex Chemicals Ltd Sp. z o. o. Other ingredients, listed below, were purchased from BrenntagPolska Sp. z o. o., Kędzierzyn - Koźle, Poland:

- stearic acid with a density of about 0.85 – 0.99 g/cm^3 and a molecular weight of 284.5 g/mol,
- zinc oxide with a density of about 5.6 g/cm^3 and a molecular weight of 81.4 g/mol,
- stabilizer AR (fenyl-β-naphthylamine): density 1.16 g/cm^3, molecular weight 219.3 g/mol,

- accelerator T (tetramethylthiuram disulfide): density 1.5 g/cm^3, molecular weight 240 g/mol.

The glycerolysate with a number average molecular weight of about 902.4 g/mol and a hydroxyl number of about 186.5 mg KOH/g was used as a plasticizer. This component was produced at the Department of Polymer Technology, Gdańsk University of Technology.

2.2. THE PREPARATION OF COMPOSITES

Five different composite specimens were prepared. Four composite samples contained different lignin contents, namely, 5, 10, 20 and 40 phr, and were coded WLI5G, WLI10G, WLI20G and WLI40G, respectively. The reference sample without lignin was also prepared (WLI0G). Before mixing, the natural rubber was annealed in air to improve the mastication process. The natural rubber was subjected to the mixing process in a BUZULUK open-roll machine (Dattaand Głowińska, 2011). Then the ingredients were added in the quantities shown in Table 1. The friction ratio between the two rolls was about 1.1:1. All composites were vulcanized at a temperature of 146 ^{o}C with the use of hydraulic press produced by ZUP Nysa. The applied pressure was ca. 5 MPa. The vulcanization temperature was chosen in accordance with the reports by Jacob et. al. (Jacobet al., 2004) and Chonkaew et. al. (Chonkaew et al., 2010).

Table 1 Composition of lignin-filled natural rubber-based composites.

2.3. CHARACTERIZATION OF THE COMPOSITES

Fourier Transform Infrared Spectroscopy was used to obtain the spectra of the samples of five composites, pure lignin, natural rubber, and glycerolysate. The measurements were carried out using a Nicolet 8700 FTIR spectrometer (Thermo Electron Corporation) with the use of ATR technique. The resolution was 4 cm^{-1}. Sixty-four scans in the wavenumber range from 4500 to 500 cm^{-1} were taken.

Scanning Electron Microscopy was used to characterize the cross-section morphology of the composites. The study was performed with the use of a Phenom G2 PRO scanning electron microscope (Phenom-World corporation) at the accelerating voltage of ca. 5 kV.

Dynamic mechanical tests were carried out with the use of a DMA Q 800 analyzer (TA Instruments). The measurements were performed in accordance with ISO 6721-1, which allowed to obtain the values of storage modulus and tangent delta (damping factor) curves. The specimens with dimensions 30 x 5 x 2 mm were analyzed at a heating rate of ca. 4 ^{o}C/min for the temperature range from -100 to 150^{o}C. The tests were performed in air, with a frequency of 1 Hz.

Thermogravimetric analysis allowed to characterize the thermal stability of the prepared composites. The measurements were carried out with the use of a NETZSCH TG 209F3 analyzer. The specimens weighing ca. 5 mg each were analyzed under nitrogen atmosphere. The temperature used ranged from 35 to 600^{o}C at a heating rate of 20 ^{o}C/min.

The mechanical properties, such as tensile strength, elongation at break, and permanent elongation after break, were determined with the use of a Zwick/Roell Z020 universal testing machine. The tests were performed in accordance with ISO 37, with the crosshead speed set to 300 mm/min and the 20 kN load cell. The dumbbell-shaped specimens of all composites were tested. The obtained results are reported as average values calculated from three samples.

The hardness measurements were performed with a Shore type A Durometer (Zwick/Roell). The circular specimens with a thickness of 6 mm were tested in accordance with the standard ISO 868. The presented results are the mean values of hardness based on ten independent measurements.

A Schob machine was used to analyze the rebound resilience of the obtained materials. Tests were performed on the circular, 6-mm thick samples in accordance with ISO 4662. The mean values calculated from ten measurements are reported for all the composites.

The density of the produced materials was determined by using an electronic analytical balance equipped with a kit for measuring the density of solids. During the single test the sample was weighed in air and in the liquid of known density, namely, methanol with a density of ca. 0.790 g/cm^3. All measurements were performed at a temperature of 23^{o}C in accordance with ISO 2781. The presented results are the mean values calculated from three independent measurements.

The abrasion resistance was investigated with the use of a Schopper-Schlobbach instrument. All specimens were circles of diameter 17 mm. Tests were performed on three samples of each material in accordance with ISO 4649. The average values were calculated from three independent measurements. The abrasiveness V (cm^3) was defined as a volume loss, and determined from equation (1):

$$V = (m_0 – m_1) * m_t / (\rho * \Delta m_w) \quad (1)$$

where: m_0 (g) and m_1 (g) are the sample mass before and after the test, respectively; m_t (g) is a theoretical loss of weight of the reference mixture (assumed value of 0.2 g); ρ (g/cm^3) is the density of tested sample; and Δm_w (g) is the average weight loss of reference mixture with the known abrasiveness (assumed value of 0.1095 g).

The swelling parameters, such as swelling index, volume fraction of rubber network, molecular weight between crosslinks, and the crosslink density, were determined by employing the equilibrium swelling method. The tests were carried out according to the descriptions presented in the literature (Abdelmouleh et al., 2007; Bahl et al., 2014; Gregorová et al., 2006; Kosikova et al., 2007). The rectangular specimens with the average dimensions 15 x 15 x 2 mm were immersed in pure toluene (purchased from POCH, Gliwice, Poland). The measurements were carried out at room temperature for 7 days (168 hours). In this time period, samples were taken out from the immersion liquid to determine the weight change. The samples were dried on paper for one minute in air, then weighted and placed again in toluene. After obtaining the equilibrium swelling state, the samples were dried in air for 7 days and then subjected to annealing at a temperature of 80°C for 3 hours (Riyajan, 2015; Stelescu et al., 2014). The swelling ratio was calculated according to the following equation (2):

$$SR = (m_a – m_b) / m_b * 100 \% \quad (2)$$

where: m_b(g) and m_a (g) are the mean weights of analyzed samples before and after swelling in the immersion liquid, respectively. In the next step of the procedure, the volume fraction of rubber network, V_{fr}(-), was calculated from equation (3):

$$V_{fr} = V_r / (V_r + V_s) = (m_r/\rho_{rr}) / (m_r/\rho_{rr} + m_s/\rho_s) \qquad (3)$$

where: V_r (cm^3) and V_s (cm^3) are the mean volumes of rubber and solvent in the swollen sample, respectively; m_r(g) and m_s (g) are the mean weights of rubber and solvent in the analyzed samples after swelling in the immersion liquid, respectively; ρ_{rr}(g/cm^3) and ρ_s (g/cm^3) are the respective densities of rubber (0.9125 g/cm^3 for natural rubber) and solvent (0.867 g/cm^3 for toluene) in the composites.

The average molecular weight between crosslinks, M_c (g/mol) was determined by using the Flory–Rehner theory according to the following equation (4):

$$M_c = \frac{-\rho_r \times V_s \times \left(V_{fr}^{\frac{1}{3}} - \frac{1}{2}V_{fr}\right)}{\ln\left(1 - V_{fr}\right) + V_{fr} + \left(\chi \times V_{fr}^{2}\right)} \qquad (4)$$

where: ρ_r(g/cm^3) means the density of lignin-rubber composites; V_s is the molar volume of solvent (106.52 cm^3/mol for toluene); and χ is the Huggins parameter, defining the interaction between the polymer and solvent (0.38 for natural rubber-toluene).

The crosslink density, v (mol/cm^3),was determined from equation (5):

$$v = \rho_r / M_c \quad (5)$$

where: ρ_r(g/cm^3) means the polymer density (lignin-rubber composite), and M_C (g/mol) is the average molecular weight of polymer.

3. RESULTS AND DISCUSSION

3.1. FOURIER TRANSFORM INFRARED (FTIR) SPECTROSCOPY

Fourier Transform Infrared analysis was used to investigate the chemical structure of the prepared lignin/rubber composites, pure lignin, natural rubber and glycerolysate used. The FTIR spectra of all composite samples (Figure 1a) demonstrated similar profiles.

Figure 1 a) FTIR spectra of the composites, pure lignin, natural rubber and glycerolysate; b) FTIR spectra of the obtained specimens for the wavenumbers ranging from 1800 to 800 cm^{-1}.

More differences were associated with the varying intensity of characteristic peaks. For the samples without the natural rubber, the characteristic wide vibration was present in all spectra in the wavelength range between 3570 and 3170 cm^{-1}, which was attributable to the stretching vibrations of hydroxyl groups derived from lignin and glycerolysate (Kubačková et al., 2013). The strong peaks with the highest intensity at 2960, 2918 and 2850 cm^{-1} correspond to the stretching vibrations of the CH_3, CH_2, CH groups from cis-1,4-polyisoprene macromolecules and glycerolysate (Riyajan, 2015) , however, the lignin particles also revealed a small shift in this wavenumber range.

For a better visibility, the FTIR spectra of samples in the wavelength range from 1800 to 800 cm^{-1} were presented in Figure 1 b. The intensive peak at 1596 cm^{-1} is attributable to the symmetric aromatic skeletal vibration indicated by lignin macromolecules (Faruket al., 2016c). Other strong bands at 1515 cm^{-1} are related to the asymetric aryl ring stretching corresponding to lignin (Faruket al., 2016c). The absorption at ca. 1445 cm^{-1} was assigned to the deformation vibrations of methyl groups –CH is related to the lignin aromatic rings, and also to the natural rubber chains (Josephet al., 2010). The band near 1377 cm^{-1} is attributable to the asymmetric vibrations of the methyl –CH groups derived from the natural rubber chain as well as glycerolysate (Dattaand Włoch, 2015). The absorption at ca. 1266 cm^{-1} was assigned to the stretching vibrations of the –C-O groups present in the phenolic rings of lignin. The peaks at ca. 1127 and 1030 cm^{-1} were attributed to the aromatic –CH groups in-plane deformation stretching originating from lignin (Faruket al., 2016c). In the case of glycerolysate, the most intensive peak at a wavenumber of 1094 cm^{-1} was attributable to the stretching vibration of the C-O group. The peak near the wavelength of ca. 839 cm^{-1} was related to the variations of –CH groups in the rubber chains (Linetal., 2015).

It is noteworthy that the intensity of characteristic peaks did not increase with the increasing amount of lignin in the composites. That can be explained by the formation of lignin agglomerates, which occurs as the amount of lignin increases. The accumulation of lignin particles results in the disturbance of the spectrum.

The interaction between the lignin units and the natural rubber chain can be explained based on the FTIR results. Jiang et al. (Jianget al., 2013) described the interaction between lignin and the poly(diallyldimethylammonium chloride) (PDADMAC) chain by comparing the shifts in the FTIR peaks corresponding to the stretching vibration of the -CH groups due to the presence of double bonds. The authors also indicated that lignin interacts with the rubber chains in the same way because of the similarity between the chain skeletons of NR and PDADMAC. In Figure 1 b, the peaks at 1515 and 1596 cm^{-1} in the spectrum of pure lignin shift to the respective locations at 1545 and 1600 cm^{-1} in the spectra of composites. A small shift from a wavenumber of 1445 cm^{-1} to 1450 cm^{-1} is also visible, which is associated with the vibration of the natural rubber chain. This little shift indicates a noncovalent interaction between the NR chain and lignin due to the adsorption of NR onto lignin. The similar results were presented by Pillai and Renneckar(Pillaiand Renneckar, 2009) , and Yang and co-workers (Yanget al., 2005).

3.2. SCANNING ELECTRON MICROSCOPY (SEM)

The cross-sections of specimens were assessed by the scanning electron microscopy in order to characterize the lignin dispersion in the composites. In addition, the SEM micrographs revealed the interaction between the lignin powder and the natural rubber matrix. Figures 2a and 2b show the specimens without lignin and those containing 5 phr of lignin, respectively. It has been demonstrated that the dispersion of this lowest quantity of lignin was satisfactory, without any visible agglomerates. Other specimens, i.e. WLI10G, WLI20G and WLI40G showed the accumulation of lignin particles. The lignin agglomerates were of irregular shape with approximate dimensions from several to several tens of micrometers (Jianget al., 2015). This finding explains the formation of hydrogen bonds between the lignin particles. It also indicates that the aggregation of lignin is unavoidable in the natural rubber matrix without additional modifications (Jianget al., 2013). Moreover, it is well known that the composites with highly dispersed filler in the rubber can bear higher stress in comparison to the composites containing the filler agglomerates. The concentration of lignin particles in the obtained composites results in a decrease in resistance (Jianget al., 2015). It is noteworthy that the observed agglomerates did not expand with increasing lignin content in the composites, however, their number increased. This can be explained by the glycerolysate content, which can suppress the accumulation of lignin particles into larger agglomerates despite the lignin polydispersity, and its propensity to form larger agglomerates with increasing lignin concentration.

Figure 2SEM images of a) reference samples, WLI0G; b) samples containing 5 phr of lignin, WLI5G; c) samples with 10 phr of lignin, WLI10G; d) samples with 20 phr of lignin, WLI20G; and e) samples with 40 phr of lignin, WLI40G.

3.3. DYNAMIC MECHANICAL ANALYSIS (DMA)

The dynamic mechanical behavior of the lignin-rubber composites was investigated with the use of dynamic mechanical analysis. The variation of the storage modulus logarithm, log E' versus temperature, and variation of tangent delta, Tan δ versus temperature were determined (Figures 3 and 4).

Figure 3 The logarithm of storage modulus (Log E’) of the lignin-rubber composites plotted versus temperature.

The characteristics of the Log E’ vs. temperature curve are typical for thermoplastic polymers with high molecular weights. The relationship between the storage modulus and temperature for the temperature range from -100 to ca. -50°C was linear. The underlying cause of this behavior is the presence of natural rubber which, at the aforementioned temperature range, occurs is the glassy state, and does not generate the reinforcing effect with the filler (Braset al., 2010). After achieving the temperature of ca. -50°C, a sharp decreasing trend was observed in the curve. This phenomenon is related to the alfa transition temperature of the natural rubber matrix. The midpoint of the decreasing curve at the temperature range from ca. -50 to ca. 0°C indicates the position of the glass transition temperature, T_g(Chonkaew et al., 2010; Geethamma et al., 2005). This point is closely associated with the relaxation of the long chain sequences of natural rubber. Cooperative motion of macromolecules induce the dissipation of energy at the temperature of maximum tan δ (Figure 4) (Abdelmouleh et al., 2007). The curve characteristics at around 0°C are related to the melting of the remaining crystalline regions in the macromolecule matrix (Gopalan Nair and Dufresne, 2003).

Figure 4 Tan δ as a function of temperature of the lignin-rubber composites.

The addition of the various amounts of lignin to the composites resulted in a decrease in the alfa transition temperature. The lowest value, i.e. ca. -44 °C was determined for the specimens containing 10 and 40 phr of lignin (Table 2). These results can be explained by impaired chain mobility due to the lignin addition, which is an obstacle for generating significant reinforcement in the composite (Chonkaew et al., 2010). The highest tan δ peak was observed in the reference sample. With increasing lignin content, the peak intensity decreased. Because the filler particles were surrounded by the rubber matrix and the hydrogen bonds formed, the movement of macromolecule chains was reduced, which resulted in the decreased intensity of the peaks (Kargarzadeh et al., 2015).

Table 2 Alfa transition temperature [°C] of the lignin-rubber composites.

3.4. THERMOGRAVIMETRIC ANALYSIS (TGA)

The thermal stability of the composites, reference sample and pure lignin was investigated with the use of thermogravimetric analysis. The measurements allowed for plotting the thermogravimetric (TGA; Figure 5) and differential thermogravimetric (DTG; Figure 6) graphs.

Figure 5 Thermogravimetric (TGA) curves for pure lignin, reference samples, and lignin-rubber composites with different lignin content.

Figure 6 Differential thermogravimetric (DTG) curves for pure lignin, reference samples, and lignin-rubber composites with different lignin content.

Both aforementioned figures present one step of thermal decomposition for all samples. The highest rate of weight loss was observed in the sample of pure lignin. The samples of lignin-rubber composites showed an increase in the weight loss rate with increasing lignin content. In comparison to the reference sample, the composites containing higher lignin levels lost weight at the lower temperature (a 5% weight loss temperature). This was caused by the effect of lignin on the thermal properties of the prepared composites. Despite the aforementioned finding, the maximum rate of mass loss for all the composites occurred at the same temperature (390^{o}C), except for the reference sample and pure lignin. For the latter two, the maximum rate of weight loss was observed at the lower temperature. In the case of temperatures of 50% and 80% weight loss, the samples displayed a similar range of maximum rate. Table 3 presents the thermal degradation characteristics for all the analyzed samples.

Table 3 Thermal degradation characteristics of the lignin-rubber composites and pure lignin, where $T_{5\%}$ is a temperature of 5% weight loss, $T_{50\%}$ is a temperature of 50% weight loss, $T_{80\%}$ is a temperature of 80% weight loss, and T_{max} is a temperature of the maximum rate of weight loss. Residue at 600^{o}C [%].

The residual weight after TGA analysis (at 600°C) increased with increasing lignin content. This resulted from the presence of the highest lignin content. The residue at 600°C comprised of ash, which consisted of organic and inorganic impurities. The impurities play an important role because they influence the thermal properties of lignin. The content of contaminants reduced the possibility of lignin softening in the composites, and decreased the quality of the filler. Moreover, due to the presence of impurities, thermal motion is hindered thereby preventing the thermal processing (Hu,2002; Kadla et al., 2002).

3.5. MECHANICAL PROPERTIES

The mechanical properties of the composites, such as tensile strength, elongation at break, and permanent elongation after break, were investigated. In order to characterize the prepared materials, their hardness, rebound resilience, density and abrasiveness were measured. Figure 7 shows the effect of varying amounts of lignin on the tensile strength of the composites.

Figure 7 Stress-strain curve of the rubber composites.

It was found that the tensile properties of the samples decreased with increasing lignin content. The composites with a low amount of filler (WLI5G and WLI10G) showed a decrease in the elongation at break and tensile strength. The specimens containing 10 phr of lignin displayed the characteristics which were similar to those of the reference sample, however, they had lower tensile strength. In the case of the samples containing 20 and 40 phr lignin, they were characterized by the higher (WLI20G) or similar (WLI40G) elongation at break, and lower tensile strength than the reference sample. The lignin admixture in the composites caused a decrease in the deformation resistance of rubber chains. Yu et al. (Yuetal., 2015) obtained similar results. Table 4 presents the results of tensile measurements.

Table 4 The effect of lignin content on the tensile properties of lignin/natural rubber composites.

The interaction between the rubber chain and the filler particles hindered the return of macromolecules to the pre-test state. For this reason, the lignin rubber composites showed an increase in the permanent elongation after break. The specimen containing 5 phr of lignin was an exception because its permanent elongation decreased.

In Table 5 the results of hardness, resilience, density and abrasiveness measurements are presented.

Table 5 The results of hardness, resilience, density and abrasiveness tests for the analyzed composites.

For the samples with 5 and 10 phr of lignin added, hardness of the analyzed composites slightly increased. In the case of the remaining filled samples, the hardness values decreased. It is known that the hardness of composites is closely related to the crosslink density (Stelescu et al., 2014). The maximum hardness at ca. 45 ^{o}Sh A was measured in the sample containing 5 phr of lignin. A decrease in hardness with increasing lignin content was correlated with the reduced crosslink density. The differences were observed in the case of the composite samples containing 5 phr of lignin. Those samples were characterized by higher hardness than the reference sample and other specimens. Thereby, the crosslink density of this particular composite displayed the greatest value.

Rebound resilience is also correlated with the crosslink density of composites. It was clearly demonstrated in this study that with increasing lignin content the crosslink density decreased (except for WLI5G), and thus the elasticity was also reduced which led to more rigid composites. Stelescu et al. obtained similar results (Stelescu et al., 2010).

Density is strictly related to the lignin amount, therefore, the highest density was measured in sample WLI40G, while the lowest, in WLI0G.

The composite with a 5 phr of lignin admixture showed the lowest abrasiveness compared to the remaining composites. This finding is clearly connected to the crosslink density of this specimen, which was the highest. For the remaining composites, the abrasion resistance decreased with increasing lignin content.

3.6. EQUILIBRIUM SWELLING PROPERTIES

The effect of lignin content on the composite network structures was investigated via the equilibrium swelling test. The following parameters were determined: the volume fraction of rubber, molecular weight between the crosslinks, crosslink density, and swelling ratio all of composites. Table 6 presents the results of those measurements.

Table 6 The results of equilibrium swelling measurements performed on the lignin-rubber composites.

With increasing lignin content the swelling ratio of the composites decreased (Table 6) in comparison to the reference specimen. The swelling ratio increased only in the case of the composites with the highest lignin content. M. Jacob et al. (Jacobet al., 2004) pointed out that the solvent diffusion mechanism in the rubber matrix is correlated with the polymer’s ability to form voids suitable for the solvent uptake. With increasing lignin content in the composites, the number of voids in the rubber matrix decreased, locking the pathways for the solvent, and thus the solvent uptake also decreased. The highest value of the swelling ratio of the specimen with a 40 phr lignin content is related to the most numerous formation of agglomerates with the highest volume. The aforementioned amount of lignin in the composite is too high for the successful hydrogen bond formation between the lignin particles and the natural rubber matrix. As a result, the lignin particles can leach out from the samples during the swelling ratio measurements, which makes the high solvent uptake possible. The swelling ratio is related to the crosslink density. (Jacobet al., 2004; Park and Cho, 2003) suggested that the maximum interaction between the rubber chain and filler, and the lowest crosslink density are characteristic for the composites with the highest admixture of lignin. The obtained results showed that the lignin content caused a decrease in the crosslink density (Table 6). Lignin in the natural rubber vulcanizates lowers the number of polysulfidic crosslinks between the rubber chains if the disulfidic and monosulfidic crosslinks remain constant (Faruket al., 2016b). The decreased amount of polysulfides lowers the hardness, resilience, abrasion resistance and tensile properties (Stelescu et al., 2010). The lignin particles mask some of the sites on the natural rubber molecules, that otherwise would have been available for crosslinking (Kumaran et al., 1978) , and cause a decrease in the network density. Due to the occurrence of masked crosslinking sites, the distance between the network nodes increases. The larger distance between the networks leads to the polymer chain tangling. The increased molecular weight between crosslinks (see Table 6) is a proof of the increased complexity of natural rubber macromolecules between the network nodes.

During the equilibrium swelling measurements the values of weight loss were recorded over time (Figure 8). The samples containing 5 and 10 phr of lignin displayed a lower weight change than the reference samples. The sample with a 5 phr lignin content showed the lowest weight loss. The two composites with the highest lignin contents displayed a higher weight loss than the reference samples. The performed measurement allowed for concluding that a low lignin content in the composites containing glycerolysate as a plasticizer, resulted in a decrease in the solvent (toluene) absorption.

Figure 8 Weight loss during the swelling measurements performed on the lignin-rubber composites.

4. CONCLUSIONS

The softwood-lignin/natural rubber composites were successfully prepared with the use of a novel plasticizer. Nowadays, the plasticizers mainly originate from the petrochemical resources. Glycerolysate used in this work is the product of the chemical recycling of polyurethanes. The results of the presented research demonstrated that the mechanical and thermal properties of softwood-lignin/natural rubber composites obtained with the use of glycerolysate as a plasticizer are similar to those of the lignin-containing composites prepared with other commercially available plasticizing agents. In addition, the data showed that the composite containing 5 phr of lignin displayed the best properties. Specimen WLI5G had the highest values of hardness and abrasiveness, and superior tensile properties. The Scanning Electron Microscopy (SEM) confirmed a positive interaction between the rubber chains and the lignin particles. The SEM images of composite WLI5G showed good dispersion of lignin, without the lignin agglomerates. The prepared four composite formulas with increasing lignin content allowed the determination of maximum lignin content in the composite that would not alter the material’s positive properties.The composite containing the highest amount of lignin (WLI40G) had the biggest and most numerous agglomeratesand, consequently, the worst mechanical (the lowest values of tensile strength, elongation after break, etc.) and thermal properties (e.g. the fastest weight loss). This observation has been confirmed by the results of swelling measurements, where sample WLI40G displayed the highest swelling ratio. The application of lignin that is the product of natural origin, and the use of the product of the chemical recycling of polyurethanes makes the described procedure eco-friendly. Its economic advantages should also be considered. Glycerolysate, used as a plasticizing agent, is less expensive than the commonly employed plasticizers derived from petrochemicals. In summary, this work is a promising development in the field of natural product utilization, and the application of the products of chemical recycling in the natural rubber matrix.

ACKNOWLEDGMENTS

The authors gratefully acknowledge receiving the samples of lignin powder used in this study from MeadWestvaco Corporation, Specialty Chemical Division, South Carolina (USA).

REFERENCES:

Abdelmouleh, M., Boufi, S., Belgacem, M.N., Dufresne, A., 2007. Short natural-fibre reinforced polyethylene and natural rubber composites: Effect of silane coupling agents and fibres loading. Compos. Sci. Technol. 67, 1627–1639. doi:10.1016/j.compscitech.2006.07.003

Alexander, M., Thachil, E.T., 2006. A comparative study of cardanol and aromatic oil as plasticizers for carbon-black-filled natural rubber. J. Appl. Polym. Sci. 102, 4835–4841. doi:10.1002/app.24811

Altenhofen Da Silva, M., Adeodato Vieira, M.G., Gomes Maumoto, A.C., Beppu, M.M., 2011. Polyvinylchloride (PVC) and natural rubber films plasticized with a natural polymeric plasticizer obtained through polyesterification of rice fatty acid. Polym. Test. 30, 478–484. doi:10.1016/j.polymertesting.2011.03.008

Bahl, K., Swanson, N., Pugh, C., Jana, S.C., 2014. Polybutadiene-g-polypentafluorostyrene as a coupling agent for lignin-filled rubber compounds. Polymer (Guildf). 55, 6754–6763. doi:10.1016/j.polymer.2014.11.008

Bjornsson, S., 2014. Advanced Control Methodology for Biomass Combustion. University of Washington.

Bras, J., Hassan, M.L., Bruzesse, C., Hassan, E.A., El-Wakil, N.A., Dufresne, A., 2010. Mechanical, barrier, and biodegradability properties of bagasse cellulose whiskers reinforced natural rubber nanocomposites. Ind. Crops Prod. 32, 627–633. doi:10.1016/j.indcrop.2010.07.018

Chakar, F.S., Ragauskas, A.J., 2004. Review of current and future softwood kraft lignin process chemistry. Ind. Crops Prod. 20, 131–141.

doi:10.1016/j.indcrop.2004.04.016

Chonkaew, W., Minghvanish, W., Kungliean, U., Rochanawipart, N., Brostow, W., 2010. Vulcanization characteristics and dynamic mechanical behavior of natural rubber reinforced with silane modified silica. J. Nanosci. Nanotechnol. 10, 2018–2024. doi:10.1166/jnn.2011.3563

Datta, J., 2010. Synthesis and Investigation of Glycolysates and Obtained Polyurethane Elastomers. J. Elastomers Plast. 42, 117–127. doi:10.1177/0095244309354368

Datta, J., Głowińska, E., 2011. Influence of cellulose on mechanical and termomechanical properties of elastoers obtained from mixtures contaning natural rubber. Polimery 61, 823–827.

Datta, J., Pasternak, S., 2005. Oligourethane glycols obtained in glycolysis of polyurethane foam as semi-finiszed products for cast urethane elastomers preparation. Polimery 50, 352–357.

Datta, J., Włoch, M., 2015. Morphology and properties of recycled polyethylene/ground tyre rubber/thermoplastic poli(ester-urethane) blands. Macromol. Res. 23, 1–10. doi:10.1007/s13233-015-3155-5

De Wild, P.J., Huijgen, W.J.J., Gosselink, R.J.A., 2014. Lignin pyrolysis for profitable lignocellulosic biorefineries. Biofuels, Bioprod. Biorefining 8, 645–657. doi:10.1002/bbb.1474

Faruk, O., Sain, M., Haghdan, S., Renneckar, S., Smith, G.D., 2016a. Lignin in Polymer Composites, Lignin in Polymer Composites. Elsevier. doi:10.1016/B978-0-323-35565-0.00001-1

Faruk, O., Sain, M., Kakroodi, A.R., 2016b. Lignin in Polymer Composites, Lignin in Polymer Composites. Elsevier. doi:10.1016/B978-0-323-35565-0.00010-2

Faruk, O., Sain, M., Stark, N.M., Yelle, D.J., Agarwal, U.P., 2016c. Lignin in Polymer Composites, Lignin in Polymer Composites. Elsevier. doi:10.1016/B978-0-323-35565-0.00004-7

Geethamma, V.G., Kalaprasad, G., Groeninckx, G., Thomas, S., 2005. Dynamic mechanical behavior of short coir fiber reinforced natural rubber composites. Compos. Part A Appl. Sci. Manuf. 36, 1499–1506. doi:10.1016/j.compositesa.2005.03.004

Gopalan Nair, K., Dufresne, A., 2003. Crab shell chitin whisker reinforced natural rubber nanocomposites. 1. Processing and swelling behavior. Biomacromolecules 4, 657–665. doi:10.1021/bm020127b

Gregorová, A., Košíková, B., Moravčík, R., 2006. Stabilization effect of lignin in natural rubber. Polym. Degrad. Stab. 91, 229–233. doi:10.1016/j.polymdegradstab.2005.05.009

Hatakeyama, H., Hatakeyama, T., 2010. Biopolymers: Lignin, Proteins, Bioactive Nanocomposites, in: Abe, A., Dusek, K., Kobayashi, S. (Eds.), . Springer Berlin Heidelberg, Berlin. doi:10.1007/12_2009_12

Holladay, J.E., White, J.F., Bozell, J.J., Johnson, D., 2007. Top Value-Added Chemicals from Biomass - Volume II?Results of Screening for Potential Candidates from Biorefinery Lignin. Evaluation II, 87. doi:10.2172/921839

Hu, T.Q., 2002. Chemical modification, properties and usage of lignin, Spronger Science and Business Media. doi:10.1017/CBO9781107415324.004

Jacob, M., Thomas, S., Varughese, K.T., 2004. Mechanical properties of sisal/oil palm hybrid fiber reinforced natural rubber composites. Compos. Sci. Technol. 64, 955–965. doi:10.1016/S0266-3538(03)00261-6

Jiang, C., He, H., Jiang, H., Ma, L., Jia, D.M., 2013. Nano-lignin filled natural rubber composites: Preparation and characterization. eXPRESSPolym. Lett. 5, 480–493.

Jiang, C., He, H., Yao, X., Yu, P., Zhou, L., Jia, D., 2015. In situ dispersion and compatibilization of lignin/epoxidized natural rubber composites: reactivity, morphology and property. J. Appl. Polym. Sci. 132, 1–10. doi:10.1002/app.42044

Jiang, C., He, H., Yao, X., Yu, P., Zhou, L., Jia, D., 2014. Self-crosslinkable lignin/epoxidized natural rubber composites. J. Appl. Polym. Sci. 131, 1–9. doi:10.1002/app.41166

Joseph, S., Appukuttan, S.P., Kenny, J.M., Puglia, D., Thomas, S., Joseph, K., 2010. Dynamic Mechanical Properties of Oil Palm Microfibril-Reinforced Natural Rubber Composites. Polymer (Guildf). 117, 1298–1308. doi:10.1002/app

Kadla, J.F., Kubo, S., Venditti, R.A., Gilbert, R.D., Compere, A.L., Griffith, W., 2002. Lignin-based carbon fibers for composite fiber applications. Carbon N. Y. 40, 2913–2920. doi:10.1016/S0008-6223(02)00248-8

Kargarzadeh, H., Sheltami, R.M., Ahmad, I., Abdullah, I., Dufresne, A., 2015. Cellulose nanocrystal reinforced liquid natural rubber toughened unsaturated polyester: Effects of filler content and surface treatment on its morphological, thermal, mechanical, and viscoelastic properties. Polymer (Guildf). 71, 51–59.

doi:10.1016/j.polymer.2015.06.045

Kopczyńska, P., Datta, J., 2016. Single-phase product obtained via crude glycerine depolymerisation of polyurethane elastomer: Structure characterisation and rheological behaviour. Polym. Int. doi:10.1002/pi.5128

Kosikova, B., Gregorova, A., Osvald, A., Krajcovicova, J., 2007. Role of Lignin Filler in Stabilization of Natural Rubber – Based Composites. J. Appl. Polym. Sci. 103, 1226–1231. doi:10.1002/app

Kubačková, J., Ferenc, J., Hudec, I., Šutý, Š., Jablonský, M., Annus, J., Preťo, J., 2013. Antioxidant properties of lignin in rubber blends. Elastomery 17, 21–27.

Kumaran, M.G., Mukhopadhyay, R., De, S.K., 1978. Effect of accelerator system and addition of lignin on the network structure of natural rubber vulcanizate. Polymer (Guildf). 19, 461–463. doi:10.1016/0032-3861(78)90258-6

Lin, Y., Chen, Y., Zeng, Z., Zhu, J., Wei, Y., Li, F., Liu, L., 2015. Effect of ZnO nanoparticles doped graphene on static and dynamic mechanical properties of natural rubber composites. Compos. Part A 70, 35–44. doi:10.1016/j.compositesa.2014.12.008

Mohapatra, S., Nando, G.B., 2014. Cardanol: a green substitute for aromatic oil as a plasticizer in natural rubber. Rsc Adv. 4, 15406–15418. doi:Doi 10.1039/C3ra46061d

Neutelings, G., 2011. Lignin variability in plant cell walls: contribution of new models. Plant Sci. 181, 379–86. doi:10.1016/j.plantsci.2011.06.012

Nikje, M.M.A., Nikrah, M., 2007. Glycerin as a new glycolysing agent for chemical recycling of cold cure polyurethane foam wastes in “split-phase” condition. Polym. Bull. 58, 411–423. doi:10.1007/s00289-006-0683-3

Park, S.J., Cho, K.S., 2003. Filler-elastomer interactions: Influence of silane coupling agent on crosslink density and thermal stability of silica/rubber composites. J. Colloid Interface Sci. 267, 86–91. doi:10.1016/S0021-9797(03)00132-2

Pillai, K. V., Renneckar, S., 2009. Cation-pi interactions as a mechanism in technical lignin adsorption to cationic surfaces. Biomacromolecules 10, 798–804. doi:10.1021/bm801284y

Riyajan, S.-A., 2015. Robust and biodegradable polymer of cassava starch and modified natural rubber. Carbohydr. Polym. 134, 267–277. doi:10.1016/j.carbpol.2015.07.038

Rogers, D., 2015. Lignin-Derived Thermosetting Vinyl Ester Resins for High Performance Applications.

Simon, D., Borreguero, A.M., De Lucas, A., Rodriguez, J.F., 2014. Glycolysis of flexible polyurethane wastes containing polymeric polyols. Polym. Degrad. Stab. 109, 115–121. doi:10.1016/j.polymdegradstab.2014.07.009

Simón, D., de Lucas, A., Rodríguez, J.F., Borreguero, A.M., 2016. Glycolysis of high resilience flexible polyurethane foams containing polyurethane dispersion polyol. Polym. Degrad. Stab. 133. doi:10.1016/j.polymdegradstab.2016.08.007

Stelescu, M., Manaila, E., Craciun, G., Dumitrascu, M., 2014. New Green Polymeric Composites Based on Hemp and Natural Rubber Processed by Electron Beam Irradiation. Sci. World J. 2014, 1–13.

Stelescu, M.D., Georgescu, M., Manaila, E., 2010. Aspects Regarding Crosslinking of a Natural Rubber Blend, in: Proceedings of the 3rd International Conference on Advanced Materials and Systems. pp. 313–318.

Vieira, M.G.A., Da Silva, M.A., Dos Santos, L.O., Beppu, M.M., 2011. Natural-based plasticizers and biopolymer films: A review. Eur. Polym. J. 47, 254–263. doi:10.1016/j.eurpolymj.2010.12.011

Yang, D., Rochette, J., Sacher, E., 2005. Spectroscopic Evidence for π-π Interaction between Poly (diallyldimethylammonium) Chloride and Multiwalled Carbon Nanotubes. J. Phys. Chem. B 109, 4481–4484.

Yu, P., He, H., Jiang, C., Wang, D., Jia, Y., Zhou, L., Jia, D.M., 2015. Reinforcing styrene butadiene rubber with lignin-novolac epoxy resin networks. eXPRESSPolym. Lett. 9, 36–48.

Figure Captions

Figure 1 a) FTIR spectra of the composites, pure lignin, natural rubber and glycerolysate; b) FTIR spectra of the obtained specimens for the wavenumbers ranging from 1800 to 800 cm^{-1}.

Figure 2SEM images of a) reference samples, WLI0G; b) samples containing 5 phr of lignin, WLI5G; c) samples with 10 phr of lignin, WLI10G; d) samples with 20 phr of lignin, WLI20G; and e) samples with 40 phr of lignin, WLI40G.

Figure 3 The logarithm of storage modulus (Log E’) of the lignin-rubber composites plotted versus temperature.

Figure 4 Tan δ as a function of temperature of the lignin-rubber composites.

Figure 5 Thermogravimetric (TGA) curves for pure lignin, reference samples, and lignin-rubber composites with different lignin content.

Figure 6 Differential thermogravimetric (DTG) curves for pure lignin, reference samples, and lignin-rubber composites with different lignin content.

Figure 7 Stress-strain curve of the rubber composites.

Figure 8 Weight loss during the swelling measurements performed on the lignin-rubber composites.

Table 1 Composition of lignin filled natural rubber-based composites.

COMPONENT	QUANTITIES OF INGREDIENTS (phr)				
	WLI0G	WLI5G	WLI10G	WLI20G	WLI40G
Natural rubber	100	100	100	100	100
Stearic acid	3	3	3	3	3
Zinc oxide	5	5	5	5	5
Stabilizer AR	1.5	1.5	1.5	1.5	1.5
Accelerator T	0.5	0.5	0.5	0.5	0.5
Glycerolysate	2	2	2	2	2
Lignin (INDULIN AT)	0	5	10	20	40
Sulphur	3	3	3	3	3

Table 2 Alfa transition temperature [^{o}C] of the lignin-rubber composites.

Composite	Alfa transition temperature T_{α} [^{o}C]
WLI0G	-38
WLI5G	-40
WLI10G	-44
WLI20G	-41
WLI40G	-43

Table 3 Thermal degradation characteristics of the lignin-rubber composites and pure lignin, where $T_{5\%}$ is a temperature of 5% weight loss, $T_{50\%}$ is a temperature of 50% weight loss, $T_{80\%}$ is a temperature of 80% weight loss, and T_{max} is a temperature of the maximum rate of weight loss. Residue at 600°C [%].

Sample	Thermal degradation characteristic [°C]				
	$T_{5\%}$	$T_{50\%}$	$T_{80\%}$	T_{max}	Residue at 600°C [%]
WLI0G	308	393	430	386	6
WLI5G	303	396	433	390	8
WLI10G	298	394	431	390	8
WLI20G	290	395	438	390	11
WLI40G	270	395	447	390	15
lignin	267	567	-	382	48

Table 4 The effect of lignin content on the tensile properties of lignin/natural rubber composites.

COMPOSITE	Tensile strength [MPa]	Elongation at break [%]	Permanent elongation after break [%]
WLI0G	16.25 ± 1.1	717 ± 12	18.1 ± 1.0
WLI5G	15.16 ± 0.4	626 ± 15	15.5 ± 1.1
WLI10G	14.22 ± 1.6	706 ± 15	18.4 ± 0.4
WLI20G	14.39 ± 0.7	733 ± 3	18.2 ± 0.5
WLI40G	8.39 ± 0.7	682 ± 26	21.9 ± 0.5

Table 5 The results of hardness, resilience, density and abrasiveness tests for the analyzed composites.

COMPOSITE	HARDNESS [°Sh A]	RESILIENCE [%]	DENSITY [g/cm^3]	ABRASIVENESS [cm^3]
WLI0G	43.6 ± 0.3	58.7 ± 2.0	0.9724 ± 0.0003	0.0899 ± 0.0080
WLI5G	45.5 ± 0.5	57.6 ± 0.8	0.9846 ± 0.0021	0.0847 ± 0.0170
WLI10G	44.3 ± 0.5	57.3 ± 0.9	0.9922 ± 0.0006	0.1179 ± 0.0143
WLI20G	41.2 ± 0.3	52.0 ± 1.1	1.0099 ± 0.0004	0.1469 ± 0.0221
WLI40G	38.3 ± 0.4	38.7 ± 0.7	1.0420 ± 0.0009	0.1999 ± 0.0487

Table 6 The results of equilibrium swelling measurements performed on the lignin-rubber composites.

COMPOSITE	SWELLING RATIO SR [%]	VOLUME FRACTION V_{fr} [-]	MOLECULAR WEIGHT BETWEEN CROSSLINKS M_C [g/mol]	CROSSLINK DENSITY $v \times 10^{-3}$ [mol/cm^3]
WLI0G	290.8 ± 3.1	0.2374 ± 0.0026	191.6 ± 2.1	5.01 ± 0.05
WLI5G	280.9 ± 0.3	0.2371 ± 0.0003	194.2 ± 0.2	5.07 ± 0.01
WLI10G	278.4 ± 0.9	0.2313 ± 0.0007	200.4 ± 0.6	4.95 ± 0.01
WLI20G	279.9 ± 1.6	0.2156 ± 0.0011	218.2 ± 1.0	4.62 ± 0.02
WLI40G	308.2 ± 2.9	0.1771 ± 0.0018	268.6 ± 2.6	3.88 ± 0.04

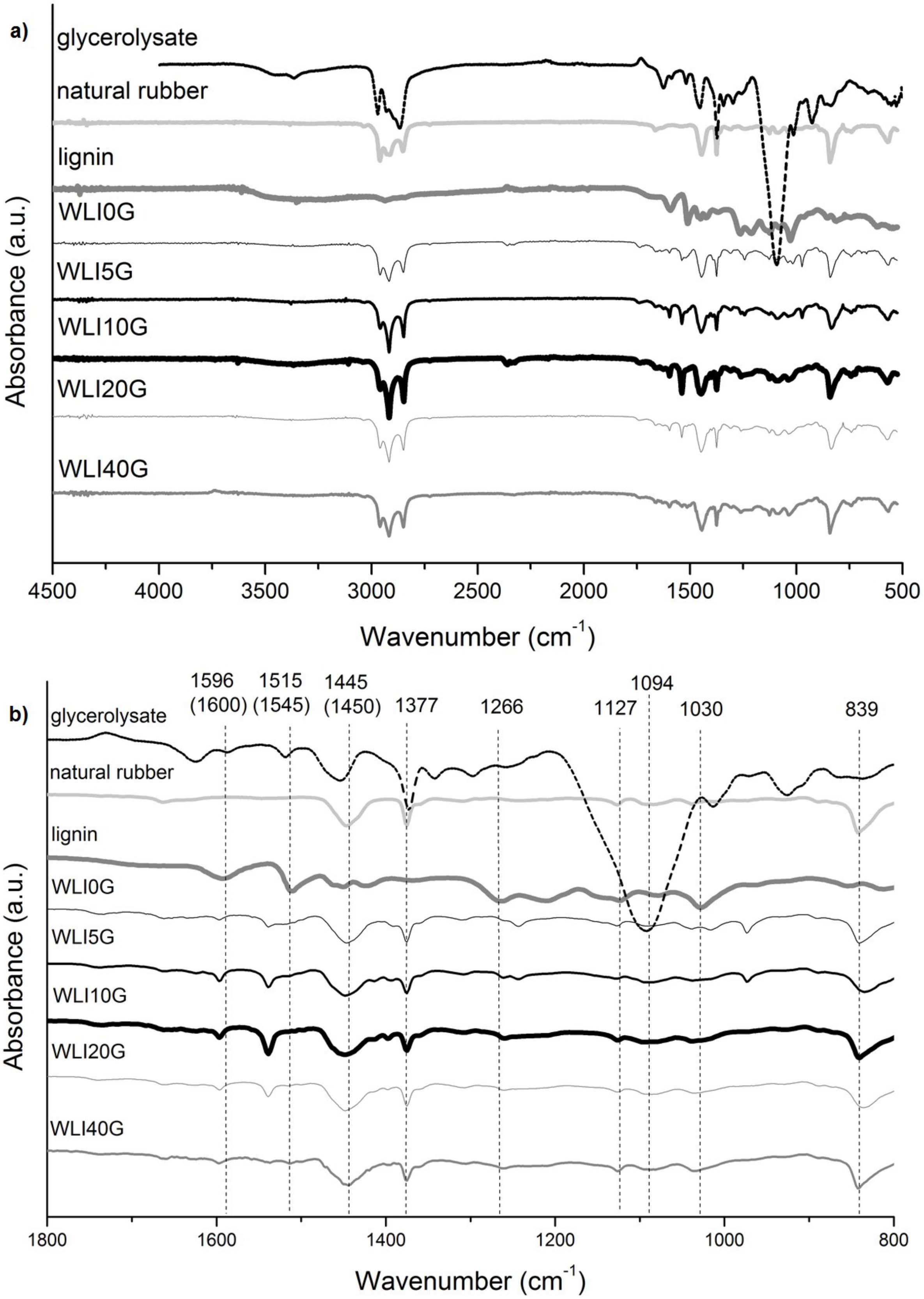
a)
glycerolysate
natural rubber
lignin
WLI0G
WLI5G
WLI10G
WLI20G
WLI40G
Absorbance (a.u.)
4500
4000
3500
3000
2500
2000
1500
1000
500
Wavenumber (cm^{-1})
b)
1596
(1600)
1515
(1545)
1445
(1450)
1377
1266
1127
1094
1030
839
glycerolysate
natural rubber
lignin
WLI0G
WLI5G
WLI10G
WLI20G
WLI40G
Absorbance (a.u.)
1800
1600
1400
1200
1000
800
Wavenumber (cm^{-1})

Figure 1

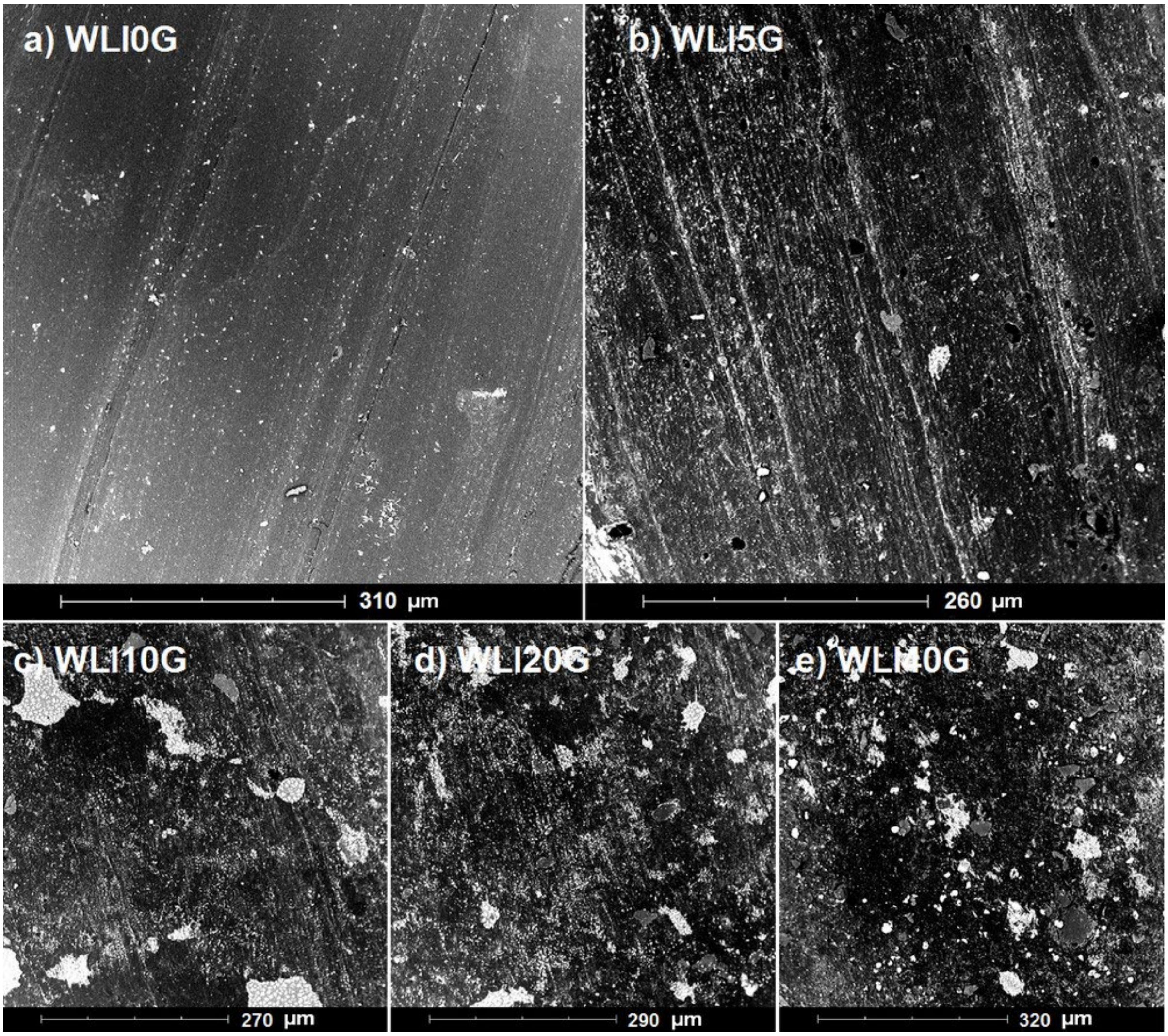
a) WLI0G
310 µm
b) WLI5G
260 µm
c) WLI10G
270 µm
d) WLI20G
290 µm
e) WLI40G
320 µm

Figure 2

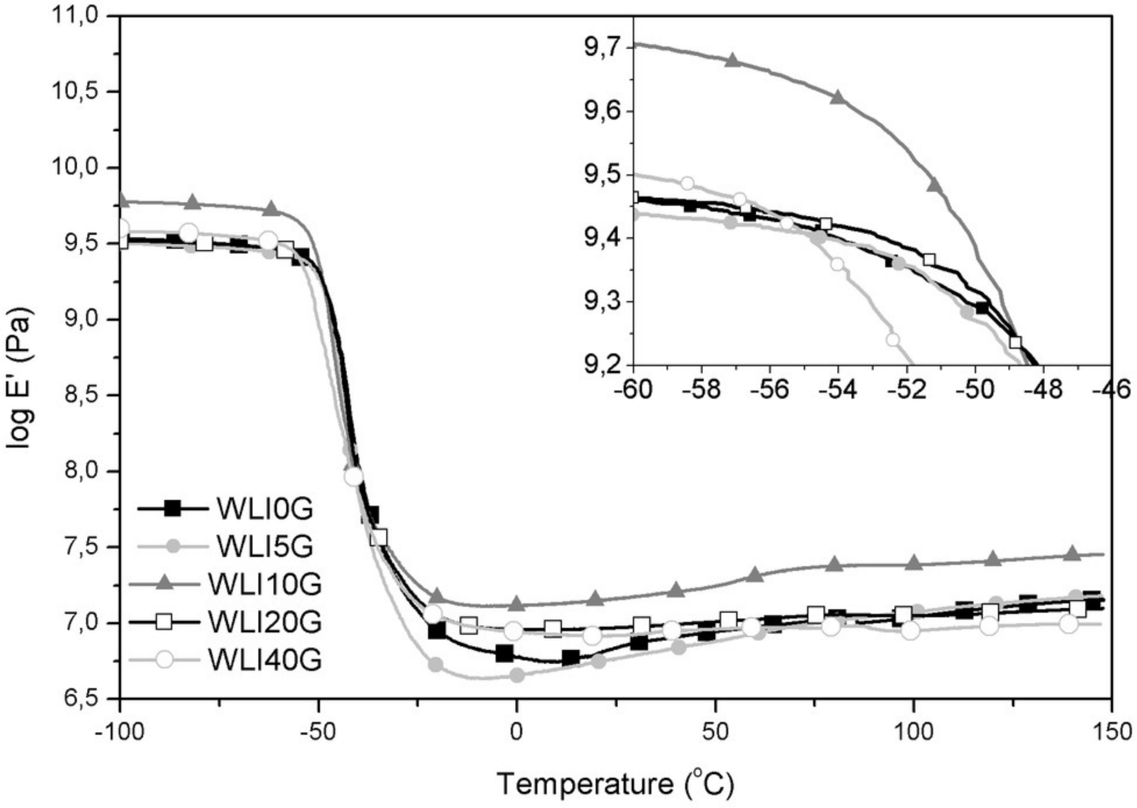

760

761 Figure 3

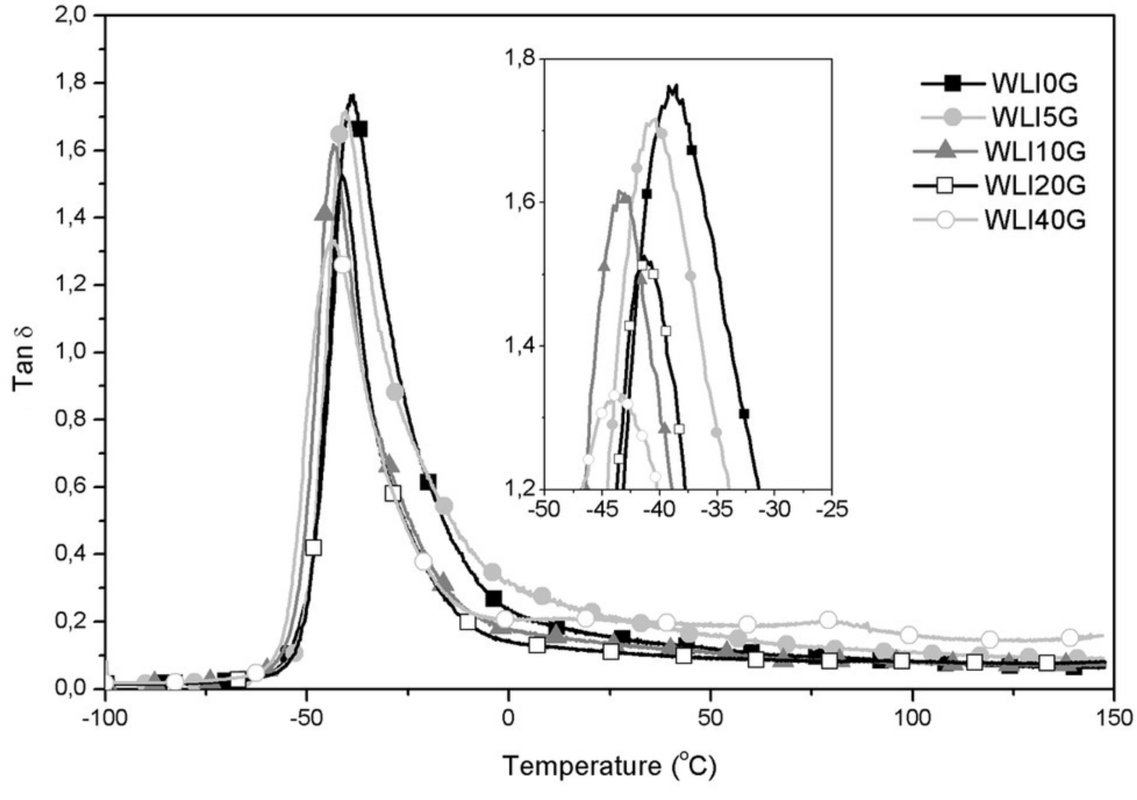

762

763 Figure 4

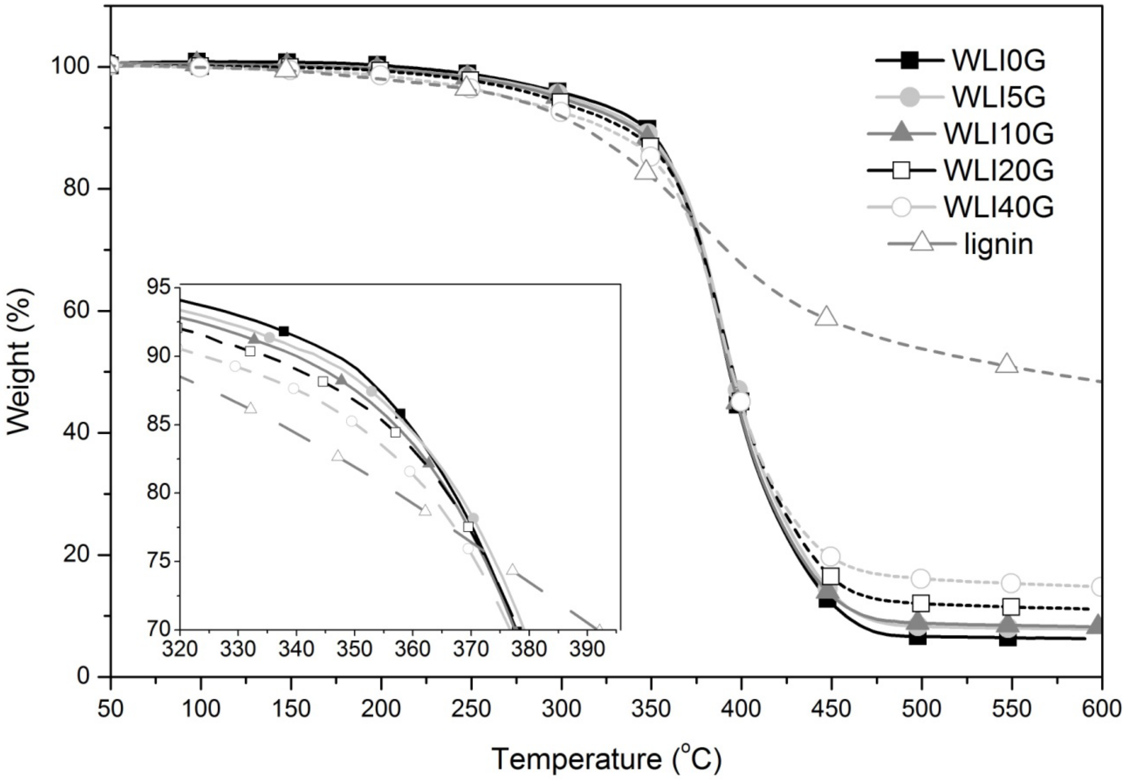

Figure 5

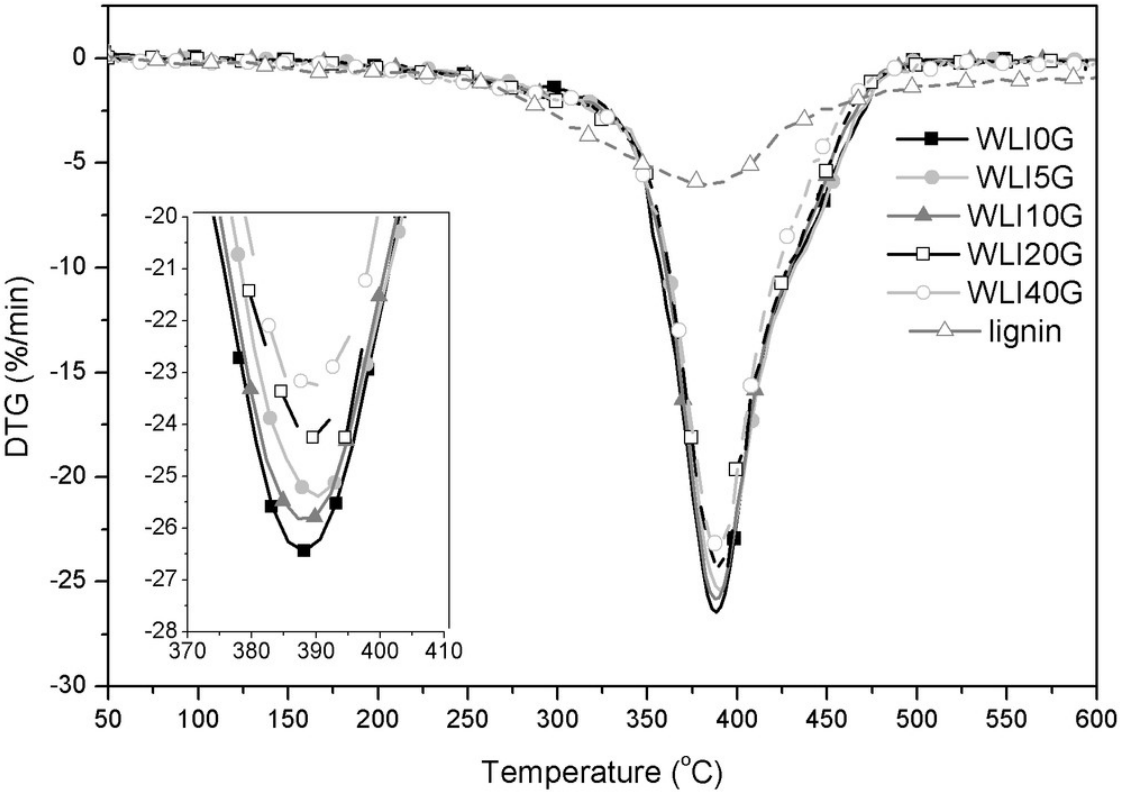

Figure 6

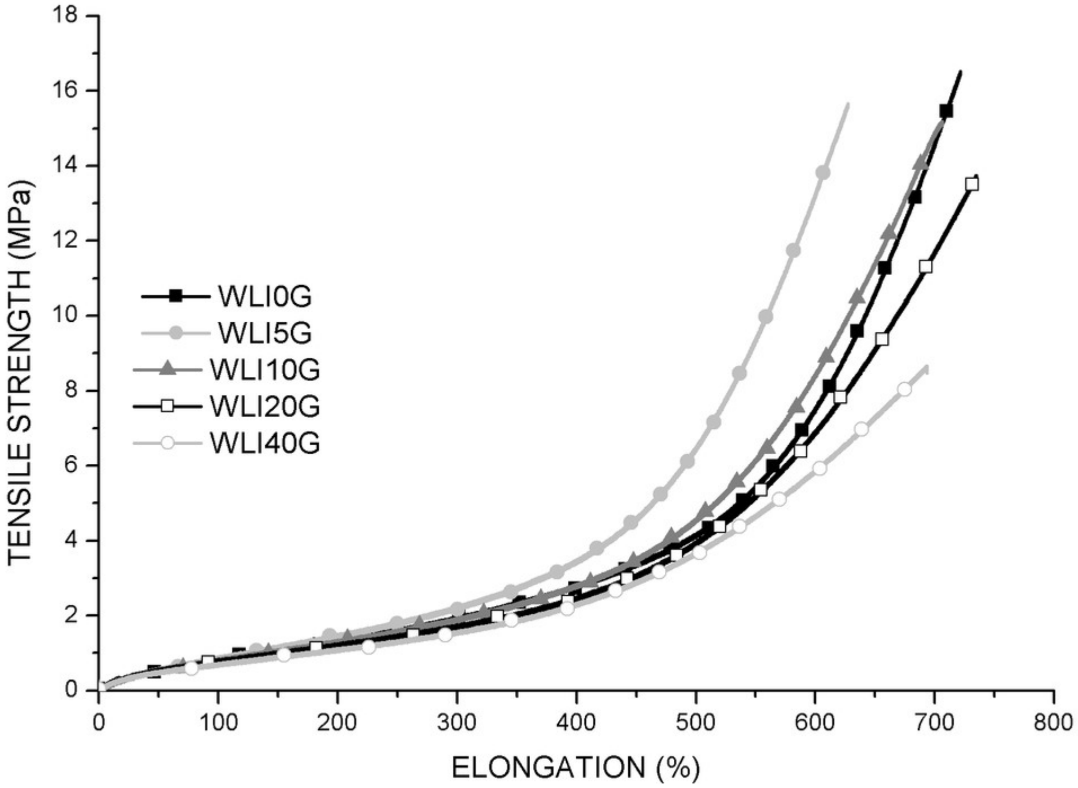

768

769 Figure 7

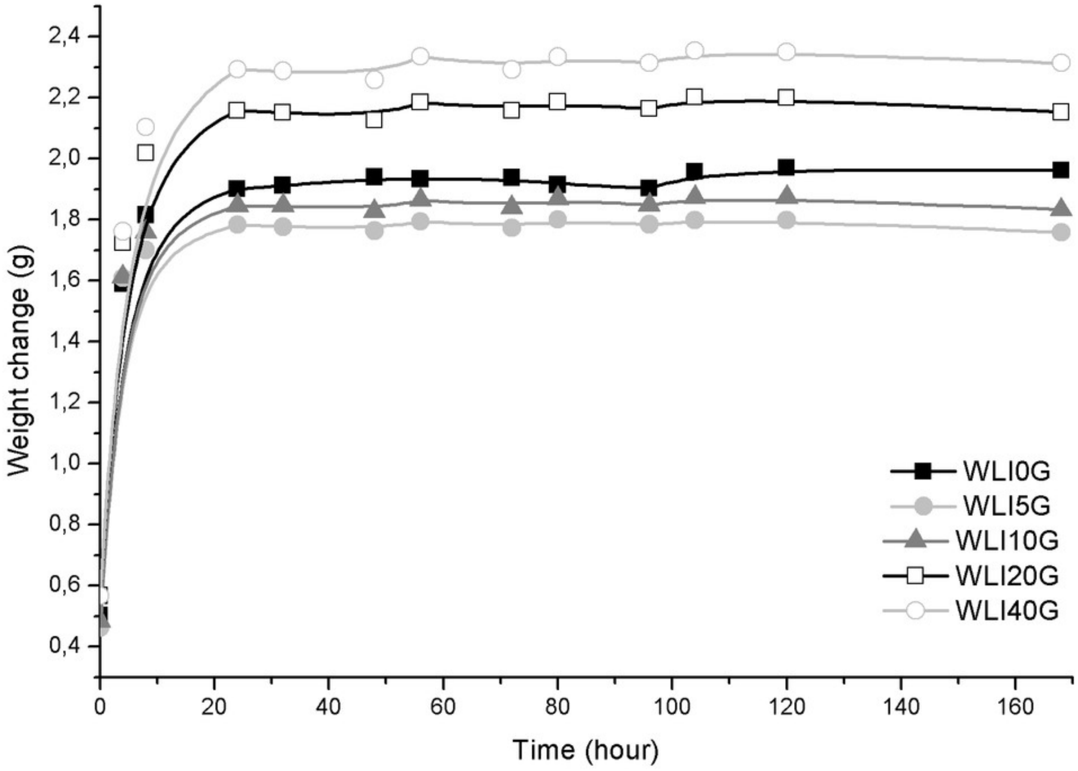

770

771 Figure 8